Neurobiology of Disease

Neurodegenerative Illness in Transgenic Mice Expressing a Transmembrane Form of the Prion Protein

Richard S. Stewart,[1] Pedro Piccardo,[2,3] Bernardino Ghetti,[2] and David A. Harris[1]

[1]Department of Cell Biology and Physiology, Washington University School of Medicine, St. Louis, Missouri 63110, [2]Division of Neuropathology, Indiana University School of Medicine, Indianapolis, Indiana 46202, and [3]Center for Biologics Evaluation and Research, Food and Drug Administration, Rockville, Maryland 20852

Although PrP^{Sc} is thought to be the infectious form of the prion protein, it may not be the form that is responsible for neuronal cell death in prion diseases. ^{Ctm}PrP is a transmembrane version of the prion protein that has been proposed to be a neurotoxic intermediate underlying prion-induced pathogenesis. To investigate this hypothesis, we have constructed transgenic mice that express L9R-3AV PrP, a mutant prion protein that is synthesized exclusively in the ^{Ctm}PrP form in transfected cells. These mice develop a fatal neurological illness characterized by ataxia and marked neuronal loss in the cerebellum and hippocampus. ^{Ctm}PrP in neurons cultured from transgenic mice is localized to the Golgi apparatus, rather than to the endoplasmic reticulum as in transfected cell lines. Surprisingly, development of the neurodegenerative phenotype is strongly dependent on coexpression of endogenous, wild-type PrP. Our results provide new insights into the cell biology of ^{Ctm}PrP, the mechanism by which it induces neurodegeneration, and possible cellular activities of PrP^{C}.

Key words: **prion; transgenic; neurodegeneration; Golgi; transmembrane; mutation**

Introduction

Prion diseases are associated with conformational conversion of an endogenous, neuronal glycoprotein (PrP^{C}) into an aggregated, β-sheet-rich isoform (PrP^{Sc}) that is infectious in the absence of nucleic acid (Prusiner, 1998; Weissmann, 2004). Because PrP^{Sc} accumulates in the brains of infected animals and humans, it has usually been assumed that this isoform is the cause of prion-induced neurodegeneration. However, several lines of evidence now suggest that, although PrP^{Sc} is the infectious form of PrP, it may not be the form directly responsible for neuronal death in prion diseases (for review, see Chiesa and Harris, 2001). Thus, there has been an attempt to identify the PrP species that initiate the neurodegenerative process. The present work focuses on one candidate for such a neurotoxic form of PrP, designated ^{Ctm}PrP.

PrP can be synthesized in the endoplasmic reticulum (ER) in three topological forms, designated ^{Sec}PrP, ^{Ntm}PrP, and ^{Ctm}PrP. ^{Sec}PrP molecules are attached to the outer leaflet of the lipid bilayer exclusively by a C-terminal glycosyl-phosphatidylinositol (GPI) anchor. ^{Ntm}PrP and ^{Ctm}PrP molecules span the lipid bilayer via a central hydrophobic region (amino acids 111–134), with either the N terminus or C terminus, respectively, on the extracytoplasmic side of the membrane (Hegde et al., 1998b; Hölscher et al., 2001; Kim et al., 2001; Stewart et al., 2001). ^{Ctm}PrP has been hypothesized to be a key pathogenic intermediate in both familial and infectiously acquired prion diseases (Hegde et al., 1999). In support of this proposition, transgenic mice expressing PrP with ^{Ctm}PrP-favoring mutations develop a scrapie-like neurological illness, but without PrP^{Sc} (Hegde et al., 1998b, 1999). However, a general role for ^{Ctm}PrP in prion diseases has been called into question by recent observations (Stewart and Harris, 2001, 2003), leaving the biological significance of this form unresolved.

A major difficulty in studying ^{Ctm}PrP is that it has not been possible to synthesize this form in either cultured cells or brain in the absence of the other two topological variants (^{Ntm}PrP and ^{Sec}PrP). To overcome this limitation, we identified nonconservative mutations in the hydrophobic core of the PrP signal peptide that markedly increased the proportion of ^{Ctm}PrP (Stewart et al., 2001; Stewart and Harris, 2003). Combining one of these mutations (L9R) with 3AV, a mutation within the transmembrane domain, to create L9R-3AV resulted in a protein that was synthesized exclusively as ^{Ctm}PrP, in both *in vitro* translation reactions and transfected cells (Stewart et al., 2001). The availability of L9R-3AV PrP provided us with the ability to analyze the properties of ^{Ctm}PrP in a cellular context in the absence of the other two topological variants (Stewart et al., 2001).

In the present study, we report on transgenic mice that express PrP carrying the L9R-3AV mutation. These Tg(L9R-3AV) mice develop a severe neurological illness accompanied by marked neuronal degeneration in several brain areas. Unexpectedly, we find that this phenotype is strongly dependent on coexpression of

Received Oct. 29, 2004; revised Feb. 15, 2005; accepted Feb. 16, 2005.

This work was supported by Department of Defense Grant DAMD-03-0531 (R.S.S.) and National Institutes of Health Grants NS40975 (D.A.H.) and P30 AG10133 (B.G.). No official endorsement of this article by the Food and Drug Administration is intended or should be inferred. We thank Charles Weissmann for *Prn-p*$^{0/0}$ mice, Richard Kascsak for 3F4 antibody, and Man-Sun Sy for 8H4 and 8B4 antibodies. We are grateful to Cheryl Adles and Michelle Kim for mouse colony maintenance and genotyping and to Rose Richardson and Constance Alyea for preparing histological specimens. We thank Mike Green for critically reading this manuscript.

Correspondence should be addressed to Dr. David A. Harris, Department of Cell Biology and Physiology, Washington University School of Medicine, 660 South Euclid Avenue, St. Louis, MO 63110. E-mail: dharris@cellbiology.wustl.edu.

DOI:10.1523/JNEUROSCI.0105-05.2005

 0270-6474/05/253469-09$15.00/0

endogenous, wild-type PrP. Our results have important implications for the cell biology of ^{Ctm}PrP, the mechanism by which it induces neurodegeneration, and possible physiological functions of PrP^{C}.

Materials and Methods

Transgenic mice. Construction of a plasmid that encodes mouse PrP containing the L9R-3AV mutation and the 3F4 antibody epitope (see Fig. 1) has been described previously (Stewart et al., 2001). The coding region of this plasmid was amplified by PCR using the following primers: GACCAGCTCGAGATGGCGAACCTTGGCTACTGG (sense); GACCAGCTCGAGTCATCCCACGATCAGGAAGAT (antisense). The amplified PCR product was digested with *Xho*I and inserted into the MoPrP.Xho vector (Borchelt et al., 1996). Purified DNA was injected into pronuclei of fertilized eggs from an F_2 cross of C57BL/6J × CBA/J F_1 parental mice. Founder animals were identified by PCR amplification of tail DNA using the following primers: AACCGAGCTGAAGCATTCTGCC (sense); CACGAGAAATGCGAAGGAACAAGC (antisense). Founders were bred to C57BL/6J × CBA/J (*Prn-p*$^{+/+}$) mice or to *Prn-p*$^{0/0}$ mice obtained from Charles Weissmann (Scripps Research Institute, West Palm Beach, FL). The latter mice, which were created on a C57BL/6J/129 background (Büeler et al., 1992), have been maintained in our laboratory by crossing onto the C57BL/6J × CBA/J background. For one line (B), transgenic animals were intercrossed to obtain progeny that were homozygous for the transgene array. The latter animals were identified by quantitative PCR. Tg(WT-E1)/*Prn-p*$^{0/0}$ and Tg(PG14-A2)/*Prn-p*$^{0/0}$ mice have been described previously (Chiesa et al., 1998). The transgenically encoded PrP in both of these lines carries the 3F4 epitope.

Animals were scored as ill if they displayed ataxia on a horizontal grid test (Chiesa et al., 1998), and they were considered to be terminal and were killed when they could no longer walk or feed themselves.

Histological analysis. Brain tissue was fixed, processed, and sectioned sagittally as described previously (Chiesa et al., 1998). Tissue sections were stained with hematoxylin and eosin. For detection of GFAP, sections were stained with an antibody from Biogenex (San Ramon, CA) at a 1:50 dilution, followed by visualization using the peroxidase–antiperoxidase (PAP) method with goat anti-rabbit IgG and rabbit PAP (Sternberger Monoclonals, Baltimore, MD). 3,3′-Diaminobenzidine was used as a chromogen. Sections were counterstained lightly with hematoxylin to reveal the localization of the cells.

Western blotting. Brain tissue was homogenized using a Teflon pestle in 10 vol of PBS containing protease inhibitors (in μg/ml: 20 PMSF, 10 leupeptin, and 10 pepstatin). Homogenates were clarified by centrifugation at 2000 × *g* for 5 min. Cultured neurons were lysed in 0.5% SDS and 50 mM Tris-HCl, pH 7.5, and the lysates were heated at 95°C for 10 min. Protein was quantified using a BCA assay (Pierce, Rockford, IL). Samples were analyzed by SDS-PAGE followed by immunoblotting with 3F4 antibody (Bolton et al., 1991) or 8H4 antibody (Zanusso et al., 1998).

Reverse transcriptase-PCR. RNA was extracted from freshly dissected forebrain or cerebellum using RNAWiz (Ambion, Austin, TX) according to the manufacturer's instructions. RNA was reverse transcribed and amplified in a one-step reaction using the Titanium kit (Clontech, Palo Alto, CA). The primers used to detect mRNA encoding transgene-derived PrP were CGCTGCGTCGCATCGGTGG (sense) and GCCATCTCGAGGTACCAC (antisense). The primers used to detect mRNA encoding endogenous PrP were GCCAAGCAGACTATCAG (sense) and CGGCTGTAGTCAGGTGTATCA (antisense). Mouse β-actin primers supplied by the manufacturer were included as an internal standard to correct for RNA input. Samples were removed every four cycles and analyzed on 8% polyacrylamide/Tris-borate EDTA gels. DNA band intensities were quantified by staining gels with SYBRGreen (Molecular Probes, Eugene, OR) and imaging with a Storm 860 phosphorimager (Amersham Biosciences, Arlington Heights, IL). The data shown were from those samples in which band intensities for both PrP and actin were within the linear range of amplification (generally 18 cycles).

Culturing and metabolic labeling of cerebellar granule cells. Primary cultures from 5-d-old pups were prepared as described previously (Miller and Johnson, 1996). Dissociated cells were resuspended in cerebellar granule neuron (CGN) medium (basal medium Eagle's, 10% dialyzed fetal bovine serum, 25 mM KCl, 2 mM glutamine, and 50 μg/ml gentamycin) and plated at a density of 500,000 cells/cm^2 in polylysine-coated plastic plates or 8-well glass chamber slides. Cells were used after 4–5 d in culture. These cultures contained >95% neurons, as assessed by staining with antibody to GFAP.

Cerebellar granule cells were labeled with 200 μCi/ml ^{35}S-Promix (Amersham Biosciences) in CGN medium lacking methionine, cysteine, and bovine serum and containing vitamin B27 supplement (Invitrogen, Carlsbad, CA). Cells were lysed in 0.5% SDS and 50 mM Tris-HCl, pH 7.5, and immunoprecipitation of PrP was performed as described previously (Drisaldi et al., 2003) using 3F4 or 8H4 antibody.

PrP membrane topology assay. Metabolically labeled cells were scraped with a pipette tip into PBS, spun at 2000 × *g* for 5 min, and resuspended in ice-cold homogenization buffer (in mM: 250 sucrose, 5 KCl, 5 $MgCl_2$, and 50 Tris-HCl, pH 7.5). Cells were lysed by 12 passages through SILASTIC tubing (inner diameter, 0.3 mm) connecting two syringes with 27 gauge needles, and nuclei were removed by centrifugation at 5000 × *g* for 10 min. Aliquots of the postnuclear supernatant were diluted into 50 mM Tris-HCl, pH 7.5, and incubated for 60 min at 4°C with 250 μg/ml proteinase K (PK) in the presence or absence of 0.5% Triton X-100. Digestion was terminated by the addition of PMSF (5 mM final concentration), and PrP was immunoprecipitated with 3F4 antibody and deglycosylated by treatment with peptide-*N*-(acetyl-β-glucosaminyl)-asparagine amidase (New England Biolabs, Beverly, MA).

Immunofluorescent labeling of brain sections and cultured neurons. Mice were perfused transcardially with 4% paraformaldehyde, after which the brains were postfixed for 3 h in the same solution and transferred to 0.1 M sodium phosphate, pH 7.2. Vibratome sections (50 μm) were incubated in blocking solution (PBS plus 2% goat serum and 0.2% Triton X-100) and stained with anti-PrP antibody 8B4 (Zanusso et al., 1998) and anti-giantin antibody (Covance, Berkeley, CA). Primary antibodies were visualized with a mixture of Alexa 488-coupled goat anti-mouse IgG and Alexa 594-coupled goat anti-rabbit IgG (Molecular Probes).

For surface labeling of cultured CGNs, cells were transferred to CGN medium containing vitamin B27 supplement instead of calf serum and stained in the living state for 10 min at 37°C with anti-PrP antibody 8H4. After rinsing with PBS, cells were fixed in 4% paraformaldehyde, 5% sucrose, and PBS for 10 min at room temperature and incubated in blocking solution (2% goat serum and PBS) for 10 min at room temperature. Cells were then stained with Alexa 488-coupled goat anti-mouse IgG, rinsed with PBS, and mounted in 50% glycerol and PBS. In some cases, cultures were incubated with phosphatidylinositol-specific phospholipase C (PIPLC) [final concentration, 1 U/ml; purified from *Bacillus thuringiensis* as described by Shyng et al. (1995)] before surface staining.

For internal labeling of cultured granule neurons, cells were fixed as above and permeabilized for 10 min at room temperature with 0.05% Triton X-100 in PBS. Cells were then incubated in blocking solution and stained with anti-PrP antibody 8B4 and anti-giantin antibody. Primary antibodies were visualized with a mixture of Alexa 488-coupled goat anti-mouse IgG and Alexa 594-coupled goat anti-rabbit IgG.

Cultured neurons and brain sections were viewed with a Zeiss (Oberkochen, Germany) LSM 510 confocal microscope equipped with an Axiovert 200 laser scanning system.

Assay of PrP^{Sc} properties. Cultures of cerebellar granule cells were labeled with ^{35}S-Promix as above. To assay detergent solubility, cells were lysed in buffer A (50 mM NaCl, 0.5% Triton X-100, 0.5% sodium deoxycholate, and 50 mM Tris-HCl, pH 7.5) at 4°C for 10 min. Lysates were first centrifuged at 14,000 × *g* for 10 min, and then the supernatant was centrifuged again at 180,000 × *g* for 40 min. PrP in supernatant and pellet fractions from the second centrifugation was immunoprecipitated and analyzed by SDS-PAGE.

To assay PK resistance, labeled cells were lysed in PK buffer (PBS plus 0.5% Triton X-100, 0.5% NP-40, 0.5% sodium deoxycholate, and 0.2% Sarkosyl), and the lysates were centrifuged at 10,000 × *g* for 10 min. Aliquots of the supernatant were treated with varying amounts of PK at 37°C for 20 min, and digestion was terminated by the addition of PMSF to a final concentration of 5 mM. PrP was then recovered by immunoprecipitation and analyzed by SDS-PAGE.

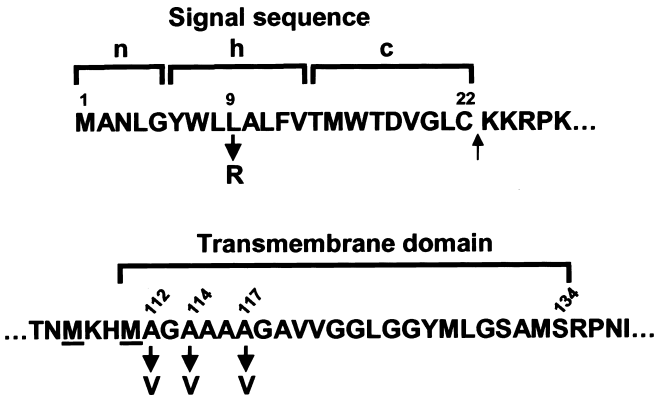

Figure 1. The amino acid sequence of murine PrP, with the L9R and 3AV mutations in the signal sequence and transmembrane domains, respectively, is shown. n, h, and c indicate, respectively, the N-terminal, hydrophobic, and C-terminal regions of the signal sequence. 3AV is the designation for the triple mutation A112V/A114V/A117V. The two underlined methionine residues at positions 108 and 111 were introduced to create an epitope for the 3F4 antibody, which allows discrimination of transgenically encoded and endogenous PrP. The upward arrow following residue 22 indicates the signal peptide cleavage site.

Table 1. Time course of neurological illness in Tg(L9R-3AV) mice

Line	Endogenous PrP (*Prn-p*)	Age at initial symptoms[a]	Age at death[a]	Number of animals
A/−	+/+	17 ± 2	21 ± 1	4[b]
B/−	+/+	172 ± 7	389 ± 12	26
B/−	0/0	>650	>650	20
B/B	+/+	38 ± 2	79 ± 3	10
B/B	0/0	72 ± 6	138 ± 10	6
C/−	+/+	85 ± 3	159 ± 5	46
C/−	+/0	104 ± 2	>300	18
C/−	0/0	144 ± 4	>300	18
D/−[c]	+/+	67	79	1

Founder mice were designated A, B, C, and D. A/−, B/−, C/−, and D/− indicate mice that are hemizygous for the transgene array. B/B indicates mice that are homozygous for the transgene array.

[a]Mean number of days ± SEM.

[b]Four of 70 offspring were transgene positive.

[c]Founder did not breed.

The conformation-dependent immunoassay was performed as described by Chiesa et al. (2003). Lysates of labeled cells prepared in buffer A were subjected to immunoprecipitation using 3F4 antibody, either with or without previous denaturation in 0.5% SDS at 95°C. The immunoprecipitated PrP was then resolved by SDS-PAGE.

Results

Spontaneous neurological illness in Tg(L9R-3AV)/*Prn-p*$^{+/+}$ mice

We introduced a murine PrP cDNA carrying the L9R-3AV mutation (Fig. 1) into the moPrP.Xho vector (Borchelt et al., 1996). This vector directs transgene expression in a pattern similar to that of endogenous PrP, with the exception that there is no expression in cerebellar Purkinje cells (Fischer et al., 1996). The mutant PrP carried an epitope for monoclonal antibody 3F4 (Bolton et al., 1991), which allowed transgenically encoded PrP to be distinguished from endogenous, murine PrP. Four founder mice (designated A–D) were obtained by pronuclear injection of fertilized oocytes from C57BL/6J × CBA/J parents (Table 1). Lines that were hemizygous for the transgene array were established from two of the founders (B and C) by breeding with nontransgenic (C57BL/6J × CBA/J) mates carrying the endogenous *Prn-p* gene.

All Tg(L9R-3AV)/*Prn-p*$^{+/+}$ mice spontaneously developed a progressive neurological illness characterized by ataxia, hindlimb paresis, and wasting (Table 1). Animals from the C line displayed an earlier onset of symptoms and shorter clinical phase before being killed than those from the B line. We intercrossed mice from the B line to produce animals homozygous for the transgene array. These animals developed symptoms shortly after weaning (38 ± 2 d), much earlier than the hemizygous B mice (172 ± 7 d), suggesting that disease onset is proportional to the expression level of mutant PrP (see below). The D founder mouse became ill at 67 d and was killed at 79 d before it could produce offspring. The A founder displayed an unusual breeding pattern. Only a small proportion (4 of 70) of transgene-positive progeny were obtained, and these were all severely runted and killed at weaning. Although this phenomenon was not investigated further, it could be attributable either to embryonic lethality of the transgene or to the presence of the transgene in only a fraction of the germ cells. In a previous study, we found that Tg(WT-E1) mice, which express wild-type PrP from the moPrP.Xho vector at levels approximately four times the endogenous PrP level, never develop clinical symptoms (Chiesa et al., 1998). Thus, the neurological illness seen in Tg(L9R-3AV) mice is related to the presence of the L9R-3AV mutation.

Neuropathology in Tg(L9R-3AV)/*Prn-p*$^{+/+}$ mice

Pathological changes were observed in the cerebellum and hippocampus of Tg(L9R-3AV)/*Prn-p*$^{+/+}$ mice from both the B and C lines. The most obvious abnormality was a marked reduction in the number of granule cells in the cerebellar cortex and a decrease in the thickness of the molecular layer (Fig. 2*A*). Loss of granule cells was most severe in the lobulus centralis, culmen, declive, uvula, and nodulus, whereas the crus II, lobulus paramedianus, and pyramis were less severely involved. Granule cells were not only fewer in number, they were also not as densely packed as normal. The molecular layer was hypercellular, and the dendrites of the Purkinje cells appeared reduced in number, although the total number of Purkinje cells appeared unchanged based on calbindin staining (data not shown). Immunohistochemical staining using anti-GFAP antibody demonstrated gliosis and astrocytic hypertrophy (Fig. 2*D*). The molecular layer displayed markedly hypertrophic Bergmann glial fibers. No spongiform changes were seen.

The hippocampus of Tg(L9R-3AV)/*Prn-p*$^{+/+}$ mice was atrophic, with reduced thickness of the pyramidal cell layer and the stratum oriens (Fig. 3*A*). The CA1 sector of the pyramidal cell layer was particularly affected. Immunohistochemical staining using anti-GFAP antibody demonstrated gliosis and astrocytic hypertrophy in the hippocampus (Fig. 3*D*).

The neurodegeneration observed in Tg(L9R-3AV)/*Prn-p*$^{+/+}$ mice was progressive, as illustrated by analysis of the cerebella of C line mice at different ages (Fig. 4). At 60 d of age, before development of symptoms, the cerebellum appeared relatively normal (Fig. 4*A*). At 85 and 99 d, after the onset of clinical symptoms, there was thinning of the granule cell and molecular layers (Fig. 4*B*,*C*). By 161 d, when animals were terminally ill, very few granule cells remained, and the cerebellum was severely atrophic (Fig. 4*D*). Our observations indicate that there is a progressive degeneration of neurons in several brain regions of Tg(L9R-3AV)/*Prn-p*$^{+/+}$ mice, although we do not rule out the possibility that there could also be effects on neuronal development and migration.

No pathological abnormalities were observed in age-matched, nontransgenic littermate mice (Figs. 2*C*,*F*, 3*C*,*F*) or in Tg(WT-E1) mice (Chiesa et al., 1998).

Neurological illness in Tg(L9R-3AV) mice is strongly dependent on coexpression of wild-type PrP

To test the effect of endogenous, wild-type PrP on the phenotype of Tg(L9R-3AV) mice, we crossed transgenic mice of the B and C lines with *Prn-p*$^{0/0}$ mice (Büeler et al., 1992) to eliminate the *Prn-p* allele. None of 20 Tg(L9R-3AV-B$^{+/-}$)/*Prn-p*$^{0/0}$ mice have shown symptoms of neurological illness, with the oldest of these living >650 d before dying of non-neurological causes (Table 1). In comparison, Tg(L9R-3AV-B$^{+/-}$)/*Prn-p*$^{+/+}$ mice first displayed symptoms at 172 d and were terminally ill by 389 d. A strong mitigating effect of eliminating the *Prn-p* allele was also evident in B line mice that were homozygous for the transgene array. Tg(L9R-3AV-B$^{+/+}$)/*Prn-p*$^{0/0}$ animals first showed symptoms at 72 d of age and became terminally ill at 138 d (Table 1). In contrast, mice homozygous for the B transgene array on the *Prn-p*$^{+/+}$ background became ill at 38 d and were terminal by 79 d. Finally, we also generated littermate Tg(L9R-3AV-C$^{+/-}$) mice on the *Prn-p*$^{+/0}$ and *Prn-p*$^{0/0}$ backgrounds. We observed that elimination of one *Prn-p* allele prolonged the onset of illness from 85 to 104 d, and elimination of both alleles delayed the onset further to 144 d. Tg(L9R-3AV-C$^{+/-}$) mice on both the *Prn-p*$^{+/0}$ and *Prn-p*$^{0/0}$ backgrounds were still alive at 300 d compared with mice on the *Prn-p*$^{+/+}$ background that were terminal by 159 d, on average. These data indicate a dose-dependent effect of endogenous PrP on the phenotype of Tg(L9R-3AV) mice.

Histological analysis confirmed the clinical results. Tg(L9R-3AV-B$^{+/-}$)/*Prn-p*$^{0/0}$ mice showed markedly improved survival of cerebellar granule cells and hippocampal pyramidal cells, as well as minimal astrogliosis, compared with age-matched Tg(L9R-3AV-B$^{+/-}$)/*Prn-p*$^{+/+}$ mice (Figs. 2*A*,*B*,*D*,*E*, 3*A*,*B*,*D*,*E*).

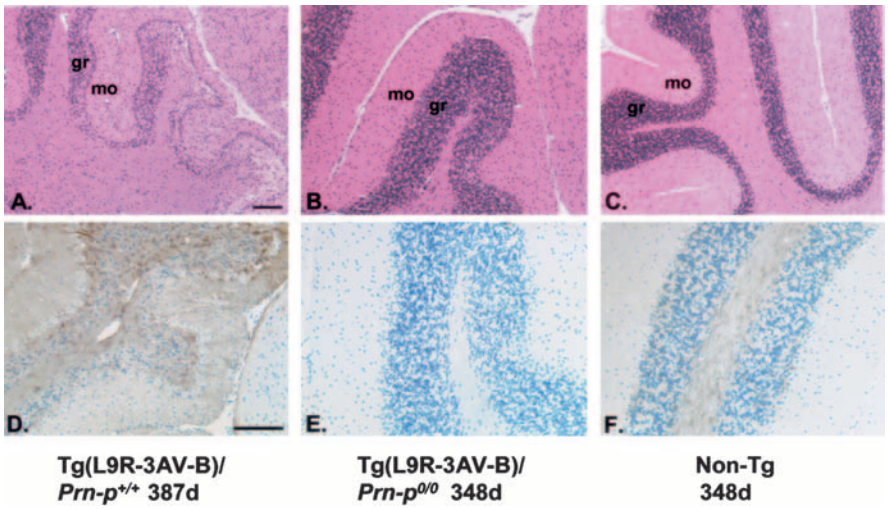

Figure 2. The histology of the cerebellum in Tg(L9R-3AV) and control mice is shown. Sections were from a Tg(L9R-3AV-B$^{+/-}$)/*Prn-p*$^{+/+}$ mouse (387 d old, symptomatic) (***A***, ***D***), a Tg(L9R-3AV-B$^{+/-}$)/*Prn-p*$^{0/0}$ mouse (348 d old, healthy) (***B***, ***E***), and a nontransgenic *Prn-p*$^{0/0}$ mouse (348 d old, healthy) (***C***, ***F***). Sections were stained with hematoxylin/eosin (***A–C***) or anti-GFAP antibody (***D–F***). gr, Granule cell layer; mo, molecular layer. Scale bars: ***A*** (for ***A–C***), ***D*** (for ***D–F***), 100 μm.

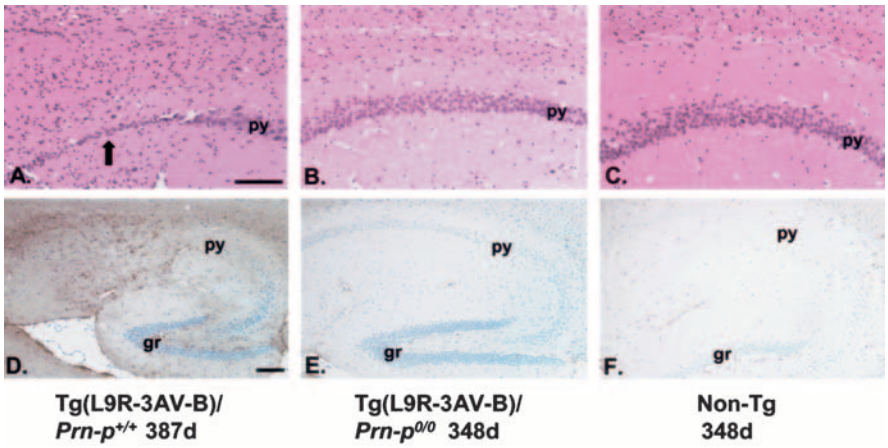

Figure 3. The histology of the hippocampus in Tg(L9R-3AV) and control mice is shown. Sections were from a Tg(L9R-3AV-B$^{+/-}$)/*Prn-p*$^{+/+}$ mouse (387 d old, symptomatic) (***A***, ***D***), a Tg(L9R-3AV-B$^{+/-}$)/*Prn-p*$^{0/0}$ mouse (348 d old, healthy) (***B***, ***E***), and a nontransgenic *Prn-p*$^{0/0}$ mouse (348 d old, healthy) (***C***, ***F***). Sections were stained with hematoxylin/eosin (***A–C***) or with anti-GFAP antibody (***D–F***). py, Pyramidal cell layer; gr, granule cell layer of the dentate gyrus. The arrow in ***A*** indicates severe loss of neurons in the pyramidal cell layer. The section shown in ***F*** was cut in a slightly different sagittal plane than those shown in ***D*** and ***E***, so the hippocampus appears larger. Scale bars: ***A*** (for ***A–C***), ***D*** (for ***D–F***), 100 μm.

Together, these results demonstrate that the neurotoxicity caused by expression of L9R-3AV PrP is dramatically accentuated by the presence of endogenous, wild-type PrP.

Transgene expression levels

Western blotting of brain homogenates from Tg(L9R-3AV) mice with 3F4 antibody revealed the presence of faint, transgene-specific PrP bands that migrated at 32–35 kDa (Fig. 5*A*, lanes 2–6). The specificity of these bands was confirmed by their absence in brain homogenates from *Prn-p*$^{0/0}$ mice (Fig. 5*A*, lane 7). The amount of L9R-3AV PrP in the runted offspring of the A founder (Fig. 5*A*, lane 2) was consistently approximately threefold higher than in mice from the B, C, or D line (Fig. 5*A*, lanes 3–5), confirming that the onset of the neurological illness in Tg(L9R-3AV) mice is correlated with the expression level of mutant PrP. However, the levels of L9R-3AV PrP observed by Western blotting in all transgenic lines were extremely low, ~1–5% of the level of endogenous PrP (data not shown) or of transgenically encoded PrP in Tg(WT-E1) mice (Fig. 5*A*, lane 1). This fact made it difficult to reliably compare the relative expression levels of the B, C, and D lines. However, our impression is that the C line expresses slightly more PrP than the B line, thus accounting for the earlier disease onset seen in the former line (Table 1).

Two kinds of experiments indicated that Western blotting significantly underestimated the amount of L9R-3AV PrP. First, reverse transcriptase (RT)-PCR was performed to estimate the levels of both transgene-derived and endogenous PrP mRNA in the brain using primer pairs specific to each species (Fig. 5*B*). Because the two PrP mRNAs were amplified in separate reactions, β-actin mRNA was used as an internal standard for RNA input to allow comparison of the PrP mRNA signals from the two reactions. The ratios of transgenic:endogenous PrP mRNA were 2.9, 1.3, and 1.4 for mice from the A, B, and C lines, respectively

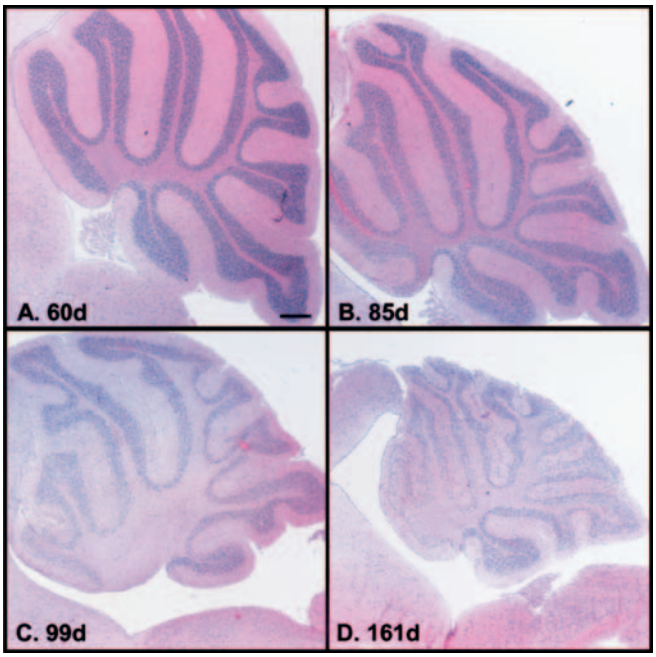

Figure 4. Neurodegeneration in the cerebellum of Tg(L9R-3AV) is progressive. Sections from Tg(L9R-3AV-C $^{+/-}$)/*Prn-p* $^{+/+}$ mice of the indicated ages were stained with hematoxylin/eosin. The 60-d-old mouse (***A***) was healthy, the 85- and 99-d-old mice (***B*** and ***C***, respectively) were symptomatic, and the 161-d-old mouse (***D***) was terminal. Scale bar: (in ***A***) ***A–D***, 100 μm.

(Fig. 5*B*, lanes 2–4). In comparison, Tg(PG14) and Tg(WT) mice (Chiesa et al., 1998) showed ratios of 1.0 and 3.6, respectively, consistent with their previously determined PrP protein expression levels of 1× and 3.6× endogenous (Fig. 5*B*, lanes 7, 8). As expected, nontransgenic *Prn-p* $^{+/+}$ mice showed only a band corresponding to endogenous PrP mRNA (Fig. 5*B*, lane 1), and nontransgenic *Prn-p* $^{0/0}$ mice showed no PrP mRNA bands (Fig. 5*B*, lane 5). Thus, we estimate that transgene mRNA is expressed in the brain at levels well above those that would be predicted based on Western blotting for PrP protein.

In a second experiment, we compared PrP protein levels in CGNs cultured from Tg(L9R-3AV-B $^{+/-}$)/*Prn-p* $^{0/0}$ and Tg(WT) mice using either immunoprecipitation or Western blotting. Immunoprecipitation of PrP from [^{35}S]methionine-labeled cells using either the 8H4 or 3F4 antibody revealed that the amount of PrP in Tg(L9R-3AV) neurons was 30% of the amount in Tg(WT) neurons (Fig. 5*C*, IP). Because the endogenous PrP level in nontransgenic mice is ~30% of the level of transgenic PrP in Tg(WT) mice (Chiesa et al., 1998), the immunoprecipitation results imply that Tg(L9R-3AV-B $^{+/-}$) mice express mutant PrP at approximately endogenous levels. In contrast, when samples from parallel cultures were subjected to Western blotting using the 8H4 or 3F4 antibody (Fig. 5*C*, WB), the amount of L9R-3AV PrP detected was only 1–5% of the amount of wild-type PrP. This discrepancy between the immunoprecipitation and Western blot results does not result from rapid metabolic turnover of L9R-3AV PrP, which has a half-life in neurons similar to that of the wild-type protein (Stewart and Harris, 2005). Rather, our results indicate that L9R-3AV PrP reacts poorly on Western blots, although it is detected efficiently by immunoprecipitation after SDS denaturation. The explanation for the poor reactivity of the mutant PrP on Western blots is unknown but may be related to masking of antibody epitopes in the protein when it is bound to the Nylon membrane either as a result of the mutations or the presence of the hydrophobic signal peptide (Stewart and Harris, 2005).

Using both Western blotting (Fig. 5*A*, lanes 3, 6) and RT-PCR (Fig. 5*B*, lanes 3, 6), we have confirmed that transgene expression levels are similar in Tg(L9R-3AV) mice on the *Prn-p* $^{0/0}$ and *Prn-p* $^{+/+}$ backgrounds. Thus, a reduction in expression of mutant PrP cannot account for the ameliorated phenotype of Tg(L9R-3AV)/*Prn-p* $^{0/0}$ mice.

Tg(L9R-3AV) neurons produce both ^{Ctm}PrP and ^{Sec}PrP

To assay the membrane topology of PrP in neurons from Tg(L9R-3AV) mice, we used primary cultures of cerebellar granule cells, which comprise one of the neuronal populations that degenerate *in vivo* in these animals. Dissociated neurons were labeled with [^{35}S]methionine, and then microsomes present in a postnuclear supernatant were subjected to protease digestion, followed by immunoprecipitation of PrP using 3F4 antibody. In this assay, fully translocated PrP (^{Sec}PrP) is completely protected from digestion, yielding a 25–27 kDa band after enzymatic deglycosylation. ^{Ctm}PrP produces a 19 kDa protected fragment, representing the lumenal and transmembrane domains of the protein. We found that microsomes from Tg(L9R-3AV-B $^{+/-}$)/*Prn-p* $^{+/+}$ neurons yielded approximately equal amounts of the 27 and 19 kDa bands, implying that these cells contained equal proportions of ^{Sec}PrP and ^{Ctm}PrP (Fig. 6, lane 5). We did not detect a 15 kDa fragment indicative of ^{Ntm}PrP. Protease treatment of microsomes in the presence of detergent eliminated both the 19 and 27 kDa bands (Fig. 6, lane 6), confirming that these species arose from protection by the microsomal membrane, rather than from intrinsic protease resistance of PrP. Identical results were obtained with neurons cultured from Tg(L9R-3AV-B $^{+/-}$)/*Prn-p* $^{0/0}$ and Tg(L9R-3AV-C $^{+/-}$)/*Prn-p* $^{+/+}$ mice (data not shown). As expected, microsomes from Tg(WT) neurons showed only a fully protected band of 25 kDa corresponding to ^{Sec}PrP (Fig. 6, lane 2). We confirmed, as reported previously (Stewart et al., 2001), that L9R-3AV PrP expressed in transfected Chinese hamster ovary (CHO) cells produces only a single, protease-protected band of 19 kDa (Fig. 6, lane 8). Thus, CHO cells synthesize the mutant protein exclusively with the ^{Ctm}PrP topology, without detectable ^{Sec}PrP. These results indicate that the L9R-3AV mutation significantly increases the ratio of ^{Ctm}PrP to ^{Sec}PrP in CGNs as well as in CHO cells, but the effect is less pronounced in the neurons.

^{Sec}PrP is localized to the cell surface, and ^{Ctm}PrP is localized to the Golgi apparatus

We used immunofluorescence staining in conjunction with phospholipase treatment to determine the subcellular distribution of ^{Ctm}PrP and ^{Sec}PrP in neurons from Tg(L9R-3AV) mice. PIPLC is a bacterial enzyme that cleaves the GPI anchor at the C terminus of PrP. PIPLC treatment is predicted to release ^{Sec}PrP but not ^{Ctm}PrP from cell membranes, because the latter form has a transmembrane anchor in addition to a GPI anchor. When we stained living (nonpermeabilized) neurons from Tg(L9R-3AV-B $^{+/-}$)/*Prn-p* $^{0/0}$ mice with any of several anti-PrP antibodies, we found that the mutant protein was distributed along the surface of neuronal processes that formed a dense meshwork in the culture (Fig. 7*A*). When cultures were treated with PIPLC, virtually all of the PrP was released from the neuronal surface (Fig. 7*B*). This result implies that most of the surface PrP has the ^{Sec}PrP topology. Identical results were obtained with neurons from Tg(L9R-3AV-B $^{+/-}$)/*Prn-p* $^{+/+}$ mice (data not shown).

Because little ^{Ctm}PrP was present on the surface, most of this form must be localized to intracellular compartments. We

stained Triton X-100-permeabilized neurons to visualize intracellular PrP. We observed that the mutant protein was present in discrete, perinuclear structures in the soma that colocalized with the Golgi marker protein giantin (Fig. 7*C–E*). Surface staining was less prominent in these permeabilized neurons, because Triton X-100 partially extracts PrP from the plasma membrane and also enhances the reactivity of cytoplasmic epitopes of Golgi-resident PrP (our unpublished observations). The distribution of PrP was identical in neurons from Tg(L9R-3AV)/*Prn-p*$^{+/+}$ and Tg(L9R-3AV)/*Prn-p*$^{0/0}$ mice from both the B and C lines (data not shown). Using immunofluorescence staining in conjunction with methods for differential permeabilization of the plasma membrane and intracellular membranes, we have demonstrated directly that PrP in the Golgi of Tg(L9R-3AV) neurons has the ^{Ctm}PrP topology (Stewart and Harris, 2005). In control experiments (data not shown), we found that wild-type PrP in neurons from nontransgenic mice was distributed primarily along the surface of neuronal processes, with little detectable intracellular staining. Thus, the ^{Ctm}PrP form of L9R-3AV PrP is concentrated in the Golgi apparatus of neurons, whereas the ^{Sec}PrP form is present on the surface of neuronal processes.

To confirm that the results obtained in cultured neurons were also applicable to brain tissue, we performed immunohistochemical staining of PrP in Triton X-100-permeabilized brain sections from Tg(L9R-3AV) mice. In the granule cell layer of the cerebellum, we found that L9R-3AV PrP was concentrated in small foci within granule cell bodies that colocalized with giantin (Fig. 7*F–H*), similar to the distribution of the protein in cultured neurons. In contrast, sections from nontransgenic control mice showed strong staining for wild-type PrP in the glomeruli surrounding granule neurons but little staining within the granule cell bodies themselves (Fig. 7*I–K*). Staining of Triton X-100-treated sections from the cerebral cortex and hippocampus of Tg(L9R-3AV) mice also revealed Golgi-localized PrP in the cell bodies of many neurons (data not shown).

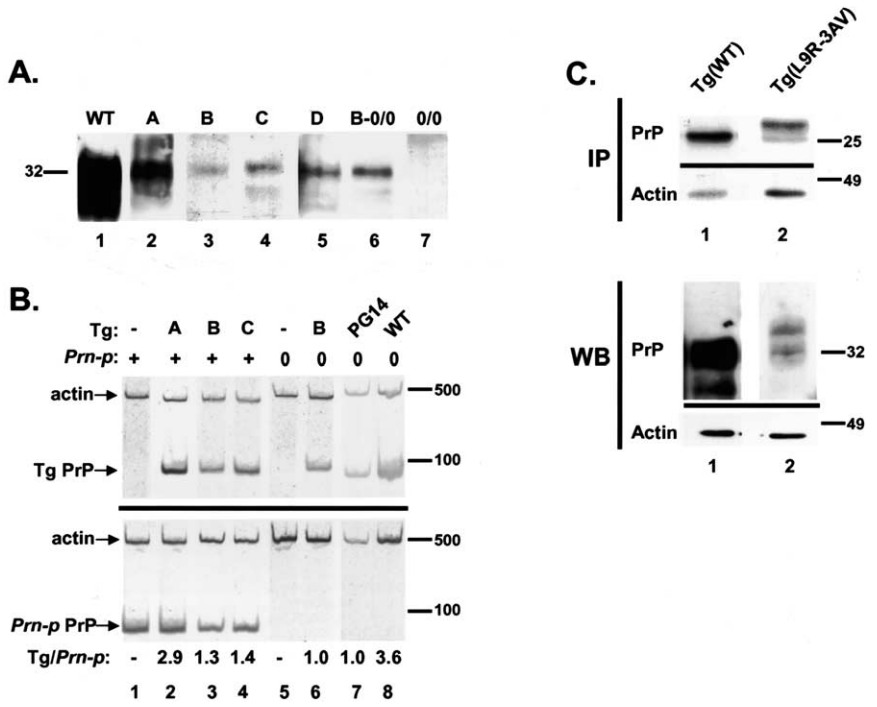

Figure 5. Expression of PrP in the brain and in cultured neurons from Tg(L9R-3AV) mice. ***A***, Brain homogenates from the following mice were analyzed by Western blotting using anti-PrP antibody 3F4: lane 1, Tg(WT); lanes 2–5, Tg(L9R-3AV $^{+/-}$)/*Prn-p*$^{+/+}$ lines A–D, respectively; lane 6, Tg(L9R-3AV $^{+/-}$)/*Prn-p*$^{0/0}$ line B; lane 7, nontransgenic *Prn-p*$^{0/0}$. Lane 1 was exposed for a shorter time than the other lanes. The molecular size marker is in kilodaltons. ***B***, RNA was extracted from the brains of mice whose transgene (Tg) and *Prn-p* status are indicated above each lane. For transgene status, A, B, and C indicate lines of Tg(L9R-3AV $^{+/-}$) mice, and a − symbol indicates that the mouse is nontransgenic. For *Prn-p* status, the + symbol indicates *Prn-p*$^{+/+}$, and the 0 symbol indicates *Prn-p*$^{0/0}$. RT-PCR was performed using primers specific for mouse β-actin and transgenically encoded PrP (top) or for mouse β-actin and endogenous (*Prn-p*-encoded) PrP (bottom). PCR products (indicated by arrows) were resolved by PAGE and stained with SYBRGreen. Tg/*Prn-p* indicates the calculated ratio of transgenically encoded to endogenous PrP. Size markers are given in nucleotides. ***C***, Duplicate cultures of cerebellar granule cells were prepared from Tg(WT) mice (lane 1) or from Tg(L9R-3AV-B $^{+/-}$)/*Prn-p*$^{0/0}$ mice (lane 2). One culture of each pair was labeled for 4 h with [^{35}S]methionine, and then PrP and actin were detected by immunoprecipitation (IP) followed by SDS-PAGE and autoradiography. The other culture of the pair was lysed, and PrP and actin were visualized by Western blotting (WB). 8H4 antibody was used to detect PrP in the experiments shown here, but similar results were obtained with 3F4 antibody (data not shown). Proteins were enzymatically deglycosylated before immunoprecipitation. In the IP experiment, the slightly slower migration of L9R-3AV PrP compared with wild-type PrP is attributable to the presence of the signal peptide on the mutant protein (Stewart and Harris, 2005).

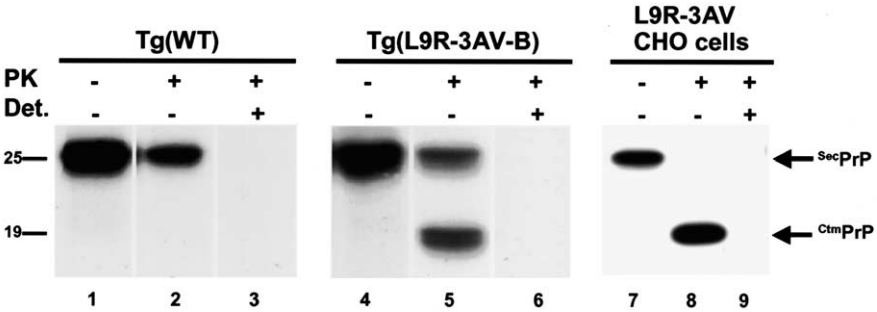

Figure 6. Neurons from Tg(L9R-3AV) mice produce both ^{Ctm}PrP and ^{Sec}PrP. CGNs cultured from Tg(WT) (lanes 1–3) or Tg(L9R-3AV-B $^{+/-}$)/*Prn-p*$^{+/+}$ (lanes 4–6) mice were labeled for 4 h with [^{35}S]methionine. CHO cells were transiently transfected with a plasmid encoding L9R-3AV PrP (lanes 7–9). Postnuclear supernatants from all cultures were then incubated with (lanes 2, 3, 5, 6, 8, 9) or without (lanes 1, 4, 7) PK in the presence (lanes 3, 6, 9) or absence (lanes 1, 2, 4, 5, 7, 8) of Triton X-100 (Det.). Proteins were then solubilized in SDS and enzymatically deglycosylated, and PrP was detected either by immunoprecipitation with 3F4 antibody (lanes 1–6) or by Western blotting with 3F4 antibody (lanes 7–9). The protease-protected forms of ^{Sec}PrP and ^{Ctm}PrP are indicated by arrows to the right of the gels.

L9R-3AV PrP does not have PrP^{Sc} properties

Previous studies have shown that ^{Ctm}PrP can cause neurodegeneration in the absence of PrP^{Sc} (Hegde et al., 1998b, 1999). We therefore tested whether PrP from Tg(L9R-3AV) mice displayed three characteristic biochemical properties of PrP^{Sc}: detergent insolubility, protease resistance, and a conformational alteration that alters antibody accessibility. As a control, we analyzed PrP from Tg(WT) and Tg(PG14) mice. Tg(PG14) mice express an insertionally mutated PrP that exhibits several PrP^{Sc}-like features (Chiesa et al., 1998). We performed these ex-

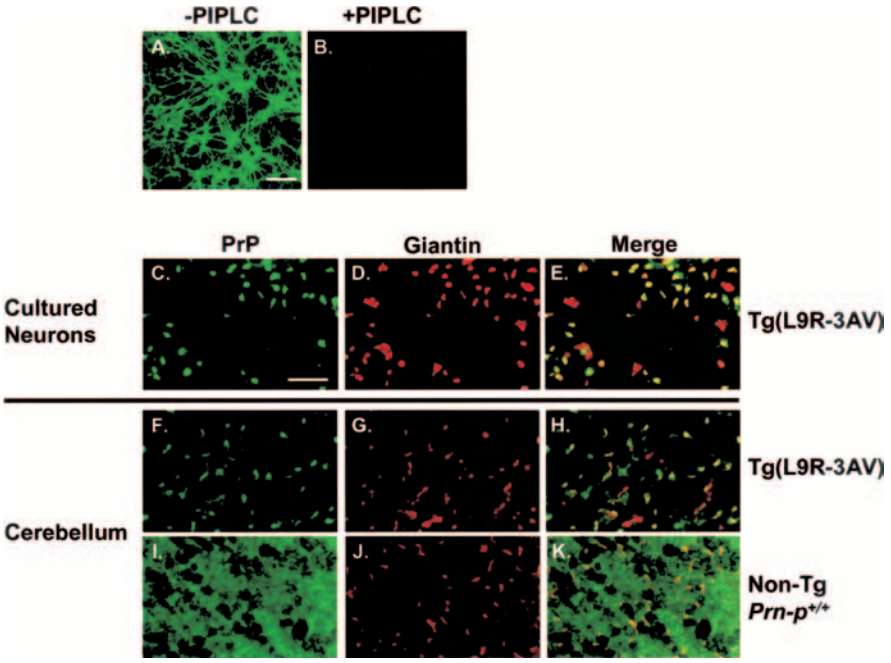

Figure 7. ^{Sec}PrP is localized to the cell surface, and ^{Ctm}PrP is localized to the Golgi apparatus. ***A***, ***B***, Cerebellar granule cells cultured from Tg(L9R-3AV-B $^{+/-}$)/*Prn-p*$^{0/0}$ mice were incubated with (***B***) or without (***A***) PIPLC and stained without permeabilization using 8H4 antibody to reveal surface PrP. ***C–E***, Cerebellar granule cells cultured from Tg(L9R-3AV-B $^{+/-}$)/*Prn-p*$^{0/0}$ mice were fixed, permeabilized with Triton X-100, and stained with anti-PrP (8B4) and anti-giantin antibodies. A green-labeled secondary antibody was used to visualize PrP (***C***), and a red-labeled secondary antibody was used to visualize giantin (***D***). ***E***, Merged image of the green and red channels demonstrating colocalization of PrP and giantin (yellow). A few cells show only red staining for giantin, presumably because they express lower levels of PrP. ***F–K***, Permeabilized vibratome sections from the cerebella of Tg(L9R-3AV-B $^{+/+}$)/*Prn-p*$^{0/0}$ (***F–H***) or nontransgenic (Non-Tg) *Prn-p*$^{+/+}$ (***I–K***) mice were stained with anti-PrP (8B4) and anti-giantin antibodies. A green-labeled secondary antibody was used to visualize PrP (***F***, ***I***) and a red-labeled secondary antibody was used to visualize giantin (***G***, ***J***). ***H***, ***K***, Merged images of the green and red channels. Images are taken from the granule cell layer of the cerebellum. Scale bars: ***A*** (for ***A***, ***B***), ***C*** (for ***C–K***), 25 μm.

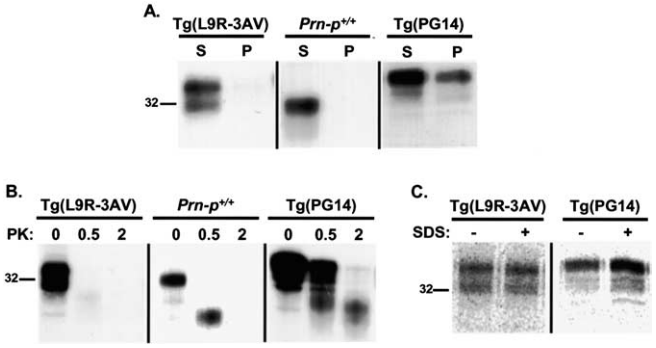

Figure 8. L9R-3AV PrP does not have PrP^{Sc} properties. ***A***, Cerebellar granule cells cultured from Tg(L9R-3AV-B $^{+/-}$)/*Prn-p*$^{+/+}$, nontransgenic *Prn-p*$^{+/+}$, or Tg(PG14) mice were labeled with [^{35}S]methionine for 4 h, and cell lysates were centrifuged at 10,000 $\times$ *g* for 10 min. The supernatant was recentrifuged at 180,000 $\times$ *g* for 45 min, and PrP in supernatant (S) and pellet (P) fractions was immunoprecipitated with 3F4 antibody [Tg(L9R-3AV), Tg(PG14)] or 8H4 antibody (*Prn-p*$^{+/+}$). ***B***, Granule cells were labeled as in ***A***. Clarified cell lysates were incubated with the indicated amounts of PK (in micrograms per milliliter) at 37°C for 20 min, after which PrP was immunoprecipitated with 3F4 antibody [Tg(L9R-3AV), Tg(PG14)] or 8H4 antibody (*Prn-p*$^{+/+}$). ***C***, Granule cells were labeled as in ***A***. PrP was immunoprecipitated from cell lysates with 3F4 antibody, either with (+) or without (−) previous denaturation in the presence of SDS.

periments by labeling cultured cerebellar neurons with [^{35}S]methionine and collecting PrP by immunoprecipitation.

In the assay for detergent insolubility (Fig. 8*A*), we found that mutant PrP in Tg(L9R-3AV) mice, like wild-type PrP in nontransgenic *Prn-p*$^{+/+}$ mice, remained in the supernatant after ultracentrifugation of a detergent lysate. In contrast, a portion of PG14 PrP was found in the pellet fraction. In the protease-resistance assay (Fig. 8*B*), we observed that L9R-3AV PrP and wild-type PrP were sensitive to digestion with low concentrations of PK under conditions in which PG14 PrP yielded a characteristic, protease-resistant fragment of 27–30 kDa. We also performed a conformation-dependent immunoassay to test the accessibility of the 3F4 epitope of PrP under native and denatured conditions (Fig. 8*C*). PrP^{Sc} and PG14 PrP, but not wild-type PrP^{C}, display a buried 3F4 epitope under native conditions (Safar et al., 1998; Chiesa et al., 2003). We found that L9R-3AV PrP (as well as wild-type PrP; data not shown) could be immunoprecipitated with 3F4 equally well in the native state and after SDS denaturation. In contrast, PG14 PrP reacted more efficiently with 3F4 after denaturation. These results indicate that L9R-3AV PrP in neurons does not display any of three biochemical signatures of PrP^{Sc}.

We also failed to detect detergent-insoluble or protease-resistant PrP when we analyzed brain homogenates from symptomatic Tg(L9R-3AV)/*Prn-p*$^{+/+}$ mice by Western blotting using either 3F4 or 8H4 antibody (data not shown). These results indicate that neither L9R-3AV PrP nor endogenous PrP is converted to a PrP^{Sc} state in clinically ill mice. We also inoculated brain homogenates from ill Tg(L9R-3AV)/*Prn-p*$^{+/+}$ mice of the B and C lines into Tga20 $^{+/0}$ indicator mice (Fischer et al., 1996) to assay for infectivity. The inoculated animals have remained healthy for >270 d, whereas Tga20 $^{+/0}$ mice inoculated with Rocky Mountain Laboratory prions become ill after 92 ± 4 d (our unpublished data). Thus, L9R-3AV PrP does not generate infectious prions.

Discussion

We have produced a neurological disorder in transgenic mice by expression of a PrP molecule that carries mutations (L9R-3AV) favoring synthesis of ^{Ctm}PrP, a transmembrane form of PrP. These mice develop severe ataxia accompanied by dramatic loss of cerebellar granule cells and hippocampal pyramidal cells. Unexpectedly, we found that development of this phenotype is strongly dependent on coexpression of endogenous, wild-type PrP. Our results provide new insights into several key issues, including the neuronal cell biology of ^{Ctm}PrP, the mechanisms of PrP-related neurotoxicity, and possible cellular activities of PrP^{C}.

Comparison of Tg(L9R-3AV) mice with other transgenic models

Hegde et al. (1998b, 1999) have previously described transgenic mice that express PrP molecules carrying mutations in the central region alone, including 3AV, that favor synthesis of ^{Ctm}PrP. These mice spontaneously develop a neurodegenerative illness characterized by ataxia and astrocytic gliosis, but without PrP^{Sc}. The mice created by Hegde et al. (1998b, 1999) differ from our Tg(L9R-3AV) mice in several important respects. First, they synthesize lower proportions of ^{Ctm}PrP (20–30%, depending on the

mutation, compared with 50% for L9R-3AV). This difference reflects the fact that mutations in the signal sequence such as L9R enhance production of ^{Ctm}PrP (Stewart and Harris, 2003). Second, the mice in the study by Hegde et al. (1998b, 1999) developed illness at much later times than our Tg(L9R-3AV) mice, when one compares lines that have an equivalent "^{Ctm}PrP index" [% ^{Ctm}PrP × Tg expression level, as defined by Hegde et al. (1999)]. We suggest that this discrepancy reflects the fact that the mice in the study by Hegde et al. (1998b, 1999) were created on the *Prn-p*$^{0/0}$ background and that introduction of the wild-type PrP allele would significantly shorten the incubation time in these animals. We hypothesize that because the mice in the study by Hegde et al. (1998b, 1999) converted proportionally more of their mutant PrP to the ^{Sec}PrP form than Tg(L9R-3AV) mice, this may be sufficient to allow disease development in the absence of endogenous, wild-type ^{Sec}PrP (see below).

Differences between transgenic neurons and transfected cells in ^{Ctm}PrP synthesis and localization

We demonstrated previously that L9R-3AV PrP is synthesized almost exclusively with the ^{Ctm}PrP topology in transiently transfected CHO, baby hamster kidney (BHK), and N2a cells (Stewart et al., 2001; Stewart and Harris, 2003). In contrast, we found that CGNs from Tg(L9R-3AV) mice express ~50% of the mutant protein as ^{Ctm}PrP and ~50% as ^{Sec}PrP. The reasons for this difference between transfected cells and granule neurons remain to be determined. One plausible explanation is that granule neurons and transformed cell lines differ in their content of protein factors that have been shown to influence the membrane topology of PrP during ER translocation (Hegde et al., 1998a; Fons et al., 2003). It is also possible that neurons possess mechanisms for selectively degrading ^{Ctm}PrP.

There is also a difference between granule neurons and transfected cells in the localization of ^{Ctm}PrP. Although most of the ^{Ctm}PrP in granule neurons from Tg(L9R-3AV) mice resides in the Golgi apparatus (this work; Stewart and Harris, 2005), most of the ^{Ctm}PrP in transfected CHO, BHK, and N2a cells expressing L9R-3AV PrP is localized to the ER (Stewart et al., 2001). We have observed that L9R-3AV PrP in fibroblasts cultured from Tg(L9R-3AV) mice is endoglycosidase H resistant (our unpublished data), arguing that the protein is trafficked to a post-ER compartment in these cells as well. Thus, factors other than cell type are likely to determine the localization of the mutant protein. It is possible that the high expression levels characteristic of transiently transfected cells cause ER retention of ^{Ctm}PrP, whereas the more physiological levels present in cells from transgenic mice allows the protein to transit further along the secretory pathway.

What is the neurotoxic species in Tg(L9R-3AV) mice, and what is its locus of action?

Tg(L9R-3AV) mice produce approximately equal proportions of mutant ^{Ctm}PrP and ^{Sec}PrP, raising the question of which of these species is responsible for the neurodegeneration seen in these animals. Two considerations argue against ^{Sec}PrP being the neurotoxic species. First, ^{Sec}PrP produced in Tg(L9R-3AV) mice behaves like wild-type PrP^{C} in terms of its cellular trafficking and biochemical properties. Second, mutations other than L9R-3AV that favor synthesis of ^{Ctm}PrP also cause neurodegeneration when expressed in transgenic mice (Hegde et al., 1998b, 1999). Thus, the L9R-3AV mutation is likely to be neurotoxic because of its effect on ^{Ctm}PrP production, rather than because of a specific alteration of the PrP amino acid sequence. It is unlikely that the neurological illness in Tg(L9R-3AV) mice is related to generation of PrP^{Sc}, because PrP from these animals does not display any of the characteristic biochemical properties of PrP^{Sc}, and the brains of these animals do not contain prion infectivity.

The localization of ^{Ctm}PrP in the Golgi apparatus raises the possibility that the neurotoxic effects of ^{Ctm}PrP may involve this organelle. The Golgi apparatus undergoes a dramatic disassembly process during apoptosis (Maag et al., 2003; Machamer, 2003). In addition, there are several caspase substrates, and at least one procaspase and a caspase inhibitor, that reside in this organelle. Thus, it is possible that ^{Ctm}PrP in the Golgi directly initiates apoptotic signals or amplifies signals that originate elsewhere in the cell.

Why is neurodegeneration in Tg(L9R-3AV) mice dependent on expression of endogenous PrP?

The most intriguing and unexpected observation to emerge from our studies is that the phenotype of Tg(L9R-3AV) mice is greatly accentuated by coexpression of endogenous, wild-type PrP. The effect of endogenous PrP is dose dependent, because Tg(L9R-3AV) mice on the *Prn-p*$^{+/0}$ background display a disease onset intermediate between that of mice on the *Prn-p*$^{0/0}$ and *Prn-p*$^{+/+}$ backgrounds. This latter result makes it unlikely that the amelioration of the phenotype associated with elimination of *Prn-p* alleles is attributable to segregation of unrelated background genes. We have ruled out several other explanations for the phenotypic disparity between mice on the *Prn-p*$^{0/0}$ and *Prn-p*$^{+/+}$ backgrounds, including differences in transgene expression level and alterations in the transgene sequence. In addition, we have confirmed that the proportion of ^{Ctm}PrP and the subcellular localization of this form are similar in CGNs of mice from both backgrounds.

Our results suggest that expression of ^{Ctm}PrP causes neurodegeneration via a process in which endogenous, wild-type PrP^{C} participates. How might this occur? Two possible models are shown in supplemental Figure 1 (available at www.jneurosci.org as supplemental material). In the simplest scheme (supplemental Fig. 1*A*, available at www.jneurosci.org as supplemental material), ^{Ctm}PrP binds to wild-type PrP^{C} (presumably in the ^{Sec}PrP form), resulting in generation of a neurotoxic signal. We also envision a second, more complex model (supplemental Fig. 1*B*, available at www.jneurosci.org as supplemental material) that takes into account a purported physiological function of PrP^{C}, namely its ability to protect neurons from various toxic insults (for review, see Roucou et al., 2004). In this scheme, PrP^{C} normally interacts with another molecule, Tr, that serves a transducer of a neuroprotective signal [supplemental Fig. 1*B* (left), available at www.jneurosci.org as supplemental material]. Because *Prn-p*$^{0/0}$ mice are phenotypically normal (Büeler et al., 1992), this neuroprotective signal would have to be nonessential under most conditions. When ^{Ctm}PrP is present along with ^{Sec}PrP, both proteins bind to Tr, causing the latter to undergo a conformational change to the Tr* state, which delivers a neurotoxic rather than a neuroprotective signal [supplemental Fig. 1*B* (right), available at www.jneurosci.org as supplemental material]. In this model, ^{Ctm}PrP is neurotoxic because it causes an inversion of the normal, neuroprotective activity of PrP^{C}. In both models, the ^{Sec}PrP component could be supplied either by endogenous, wild-type PrP or less efficiently by transgenically encoded L9R-3AV PrP if it were present in sufficient amounts. This hypothesis would explain why deleting the *Prn-p* gene ameliorated but did not completely prevent development of neurological symptoms in Tg(L9R-3AV-C$^{+/-}$)/*Prn-p*$^{0/0}$ and Tg(L9R-3AV-B$^{+/+}$)/*Prn-p*$^{0/0}$ mice. In these animals, the amount of

mutant ^{Sec}PrP may be sufficient to transmit the neurotoxic signal in the absence of endogenous ^{Sec}PrP. The fact that ^{Ctm}PrP is concentrated in the Golgi apparatus of neurons, whereas ^{Sec}PrP is found primarily on the cell surface, does not mitigate against a physical interaction of the two proteins, because ^{Sec}PrP must transit the Golgi on its way to the cell surface.

A new view of the role of ^{Ctm}PrP in prion biology

In this study, we demonstrate that ^{Ctm}PrP-associated neurodegeneration is highly dependent on the presence of wild-type PrP^{C}. This observation potentially connects the toxic activity of ^{Ctm}PrP to the normal, physiological function of PrP^{C}. There are several other situations in which expression of PrP^{C} in target neurons appears to be essential for conferring sensitivity to PrP-related neurotoxic insults (Brown et al., 1994; Brandner et al., 1996; Mallucci et al., 2003; Solforosi et al., 2004). Each of these situations could conceivably reflect the operation of a neurotoxic, PrP^{C}-dependent signaling pathway similar to the one we postulate is activated by ^{Ctm}PrP. Interestingly, the ability of PrP^{C} to accentuate the phenotype of Tg(L9R-3AV) mice appears to be the inverse of its ability to rescue the neurodegenerative phenotype of transgenic mice that ectopically express Doppel (Moore et al., 2001; Rossi et al., 2001) and N-terminally truncated PrP (Shmerling et al., 1998). It will be of great interest to determine whether these two contrasting activities of PrP^{C} are related and, if so, what molecular mechanisms account for whether PrP^{C} delivers a neurotoxic or neuroprotective signal.

References

Bolton DC, Seligman SJ, Bablanian G, Windsor D, Scala LJ, Kim KS, Chen CM, Kascsak RJ, Bendheim PE (1991) Molecular location of a species-specific epitope on the hamster scrapie agent protein. J Virol 65:3667–3675.

Borchelt DR, Davis J, Fischer M, Lee MK, Slunt HH, Ratovitsky T, Regard J, Copeland NG, Jenkins NA, Sisodia SS, Price DL (1996) A vector for expressing foreign genes in the brains and hearts of transgenic mice. Genet Anal Biomol Eng 13:159–163.

Brandner S, Isenmann S, Raeber A, Fischer M, Sailer A, Kobayashi Y, Marino S, Weissmann C, Aguzzi A (1996) Normal host prion protein necessary for scrapie-induced neurotoxicity. Nature 379:339–343.

Brown DR, Herms J, Kretzschmar HA (1994) Mouse cortical cells lacking cellular PrP survive in culture with a neurotoxic PrP fragment. NeuroReport 5:2057–2060.

Büeler H, Fischer M, Lang Y, Fluethmann H, Lipp H-P, DeArmond SJ, Prusiner SB, Aguet M, Weissmann C (1992) Normal development and behavior of mice lacking the neuronal cell-surface PrP protein. Nature 356:577–582.

Chiesa R, Harris DA (2001) Prion diseases: what is the neurotoxic molecule? Neurobiol Dis 8:743–763.

Chiesa R, Piccardo P, Ghetti B, Harris DA (1998) Neurological illness in transgenic mice expressing a prion protein with an insertional mutation. Neuron 21:1339–1351.

Chiesa R, Piccardo P, Quaglio E, Drisaldi B, Si-Hoe SL, Takao M, Ghetti B, Harris DA (2003) Molecular distinction between pathogenic and infectious properties of the prion protein. J Virol 77:7611–7622.

Drisaldi B, Stewart RS, Adles C, Stewart LR, Quaglio E, Biasini E, Fioriti L, Chiesa R, Harris DA (2003) Mutant PrP is delayed in its exit from the endoplasmic reticulum, but neither wild-type nor mutant PrP undergoes retrotranslocation prior to proteasomal degradation. J Biol Chem 278:21732–21743.

Fischer M, Rülicke T, Raeber A, Sailer A, Moser M, Oesch B, Brandner S, Aguzzi A, Weissmann C (1996) Prion protein (PrP) with amino-proximal deletions restoring susceptibility of PrP knockout mice to scrapie. EMBO J 15:1255–1264.

Fons RD, Bogert BA, Hegde RS (2003) Substrate-specific function of the translocon-associated protein complex during translocation across the ER membrane. J Cell Biol 160:529–539.

Hegde RS, Voigt S, Lingappa VR (1998a) Regulation of protein topology by *trans*-acting factors at the endoplasmic reticulum. Mol Cell 2:85–91.

Hegde RS, Mastrianni JA, Scott MR, Defea KA, Tremblay P, Torchia M, DeArmond SJ, Prusiner SB, Lingappa VR (1998b) A transmembrane form of the prion protein in neurodegenerative disease. Science 279:827–834.

Hegde RS, Tremblay P, Groth D, DeArmond SJ, Prusiner SB, Lingappa VR (1999) Transmissible and genetic prion diseases share a common pathway of neurodegeneration. Nature 402:822–826.

Hölscher C, Bach UC, Dobberstein B (2001) Prion protein contains a second endoplasmic reticulum targeting signal sequence located at its C terminus. J Biol Chem 276:13388–13394.

Kim SJ, Rahbar R, Hegde RS (2001) Combinatorial control of prion protein biogenesis by the signal sequence and transmembrane domain. J Biol Chem 276:26132–26140.

Maag RS, Hicks SW, Machamer CE (2003) Death from within: apoptosis and the secretory pathway. Curr Opin Cell Biol 15:456–461.

Machamer CE (2003) Golgi disassembly in apoptosis: cause or effect? Trends Cell Biol 13:279–281.

Mallucci G, Dickinson A, Linehan J, Klohn PC, Brandner S, Collinge J (2003) Depleting neuronal PrP in prion infection prevents disease and reverses spongiosis. Science 302:871–874.

Miller TM, Johnson Jr EM (1996) Metabolic and genetic analyses of apoptosis in potassium/serum-deprived rat cerebellar granule cells. J Neurosci 16:7487–7495.

Moore RC, Mastrangelo P, Bouzamondo E, Heinrich C, Legname G, Prusiner SB, Hood L, Westaway D, DeArmond SJ, Tremblay P (2001) Doppel-induced cerebellar degeneration in transgenic mice. Proc Natl Acad Sci USA 98:15288–15293.

Prusiner SB (1998) Prions. Proc Natl Acad Sci USA 95:13363–13383.

Rossi D, Cozzio A, Flechsig E, Klein MA, Rulicke T, Aguzzi A, Weissmann C (2001) Onset of ataxia and Purkinje cell loss in PrP null mice inversely correlated with Dpl level in brain. EMBO J 20:694–702.

Roucou X, Gains M, LeBlanc AC (2004) Neuroprotective functions of prion protein. J Neurosci Res 75:153–161.

Safar J, Wille H, Itrri V, Groth D, Serban H, Torchia M, Cohen FE, Prusiner SB (1998) Eight prion strains have PrP^{Sc} molecules with different conformations. Nat Med 4:1157–1165.

Shmerling D, Hegyi I, Fischer M, Blättler T, Brandner S, Götz J, Rülicke T, Flechsig E, Cozzio A, von Mering C, Hangartner C, Aguzzi A, Weissmann C (1998) Expression of amino-terminally truncated PrP in the mouse leading to ataxia and specific cerebellar lesions. Cell 93:203–214.

Shyng SL, Moulder KL, Lesko A, Harris DA (1995) The N-terminal domain of a glycolipid-anchored prion protein is essential for its endocytosis via clathrin-coated pits. J Biol Chem 270:14793–14800.

Solforosi L, Criado JR, McGavern DB, Wirz S, Sanchez-Alavez M, Sugama S, DeGiorgio LA, Volpe BT, Wiseman E, Abalos G, Masliah E, Gilden D, Oldstone MB, Conti B, Williamson RA (2004) Cross-linking cellular prion protein triggers neuronal apoptosis *in vivo*. Science 303:1514–1516.

Stewart RS, Harris DA (2001) Most pathogenic mutations do not alter the membrane topology of the prion protein. J Biol Chem 276:2212–2220.

Stewart RS, Harris DA (2003) Mutational analysis of topological determinants in prion protein (PrP) and measurement of transmembrane and cytosolic PrP during prion infection. J Biol Chem 278:45960–45968.

Stewart RS, Harris DA (2005) A transmembrane form of the prion protein is localized in the Golgi apparatus of neurons. J Biol Chem, in press.

Stewart RS, Drisaldi B, Harris DA (2001) A transmembrane form of the prion protein contains an uncleaved signal peptide and is retained in the endoplasmic reticulum. Mol Biol Cell 12:881–889.

Weissmann C (2004) The state of the prion. Nat Rev Microbiol 2:861–871.

Zanusso G, Liu D, Ferrari S, Hegyi I, Yin X, Aguzzi A, Hornemann S, Liemann S, Glockshuber R, Manson JC, Brown P, Petersen RB, Gambetti P, Sy MS (1998) Prion protein expression in different species: analysis with a panel of new mAbs. Proc Natl Acad Sci USA 95:8812–8816.